Inorganic Chemistry
Article

Breaking the Cycle: Impact of Sterically-Tailored Tetra(pyrazolyl)lutidines on the Self-Assembly of Silver(I) Complexes

Tyler J. Morin, Andrew Merkel, Sergey V. Lindeman, and James R. Gardinier*

Department of Chemistry, Marquette University, Milwaukee, Wisconsin 53201-1881

A improved preparation of the pentadentate ligand $\alpha,\alpha,\alpha',\alpha'$-tetra(pyrazolyl)lutidine, **pz$_4$lut**, and the syntheses of three new alkyl-substituted pyrazolyl derivatives **pz$^{4'}_4$lut** (pz$^{4'}$ = 4-methylpyrazolyl), **pz*$_4$lut** (pz* = 3,5-dimethyl-pyrazolyl), and **pz$^{DIP}_4$lut** (pz^{DIP} = 3,5-diisopropylpyrazolyl) are described. The silver(I) complexes of these ligands were studied to ascertain the impact of pyrazolyl substitution, if any, on their binding modes and on solubility issues. In the solid state, [Ag(**pz$_4$lut**)](BF$_4$) (**1**), [Ag(**pz$^{4'}_4$lut**)](BF$_4$) (**2**), and [Ag(**pz*$_4$lut**)](BF$_4$) (**3**) give cyclic dications as a result of two ligands sandwiching two silver centers where each ligand binds the metals through only pyrazolyl nitrogen donors. This cyclic motif is similar to those observed in the silver complexes of tetra(pyridyl)lutidine **PY5-R** derivatives (where the central pyridyl does not bind) and in related tetra(pyrazolyl)-*m*-xylene complexes. While suitable single crystals of [Ag(**pz$^{DIP}_4$lut**)](BF$_4$) (**4**) could not be obtained, those of [Ag(**pz$^{DIP}_4$lut**)](OTf) (**5**) showed infinite polymeric chains secured via silver-bound μ-κ^2N$_{pz}$,κ^2N$_{pz}$-ligands. The different binding mode of the latter ligand versus the former three is likely due to unfavorable steric interactions between the bulky *iso*-propyl (pyrazolyl) substituents and the central pyridyl rings of hypothetical cyclic architectures. The combined electrospray ionization mass spectrometry (ESI(+)-MS), variable-temperature NMR (VT NMR), and diffusion pulsed field-gradient spin−echo (PFGSE) NMR data indicate that the solid state structures of each **1**−**5** are neither retained nor static in CD$_3$CN, rather the cations are monomeric in solution.

Introduction

There is current interest in the coordination chemistry of simple AE$_4$ pentadentate ligands capable of occupying one axial (A) and four equatorial (E) positions about a given transition metal center[1] considering that systems capable of mediating spectacular organic transformations such as alkane oxidation have been identified.[2] As is typical in coordination chemistry of other ligands, silver(I) complexes of pentadentate ligands could serve as useful reagents for metathesis reactions and possibly for oxidation chemistry.[3] For the former purpose, the chemistry of two silver(I) **PY5-R** derivatives (Figure 1) was recently reported by Huang and

co-workers.[4] Two complexes of the type [Ag(**PY5** or **PY5-OMe**)](*p*-CH$_3$C$_6$H$_4$SO$_3$) were found by a combination of NMR studies, electrospray ionization ESI(+) mass spectral data, to be involved in a solution equilibrium (right of Figure 1) where the limiting structures, the cyclic bimetallic dication or the κ^3- monocation (depending on whether or not PPh$_3$ was added prior to crystallization), were verified by single crystal X-ray diffraction. We recently communicated[5] an initial survey of first-row transition metal coordination chemistry of the pentadentate ligand, $\alpha,\alpha,\alpha',\alpha'$-tetra-(pyrazolyl)lutidine (**pz$_4$lut**, Figure 2). During the course of our continuing investigations, we found that some silver(I) complexes of **pz$_4$lut** (with non-coordinating tetrafluoroborate or triflate counterions) exhibited surprisingly low solubility in polar solvents such as CH$_3$OH and CH$_3$CN, solvents in which most silver(I) complexes (including the **PY5-R** derivatives) are soluble. This observation and the interesting results reported for **PY5** derivatives prompted us to more carefully examine the properties of this silver(I) **pz$_4$lut** complex and some alkyl-substituted derivatives. Herein we report on an improved preparation of **pz$_4$lut**, the syntheses of three new alkylpyrazolyl-substituted derivatives **pz$^{4'}_4$lut** (pz$^{4'}$ = 4-methylpyrazolyl), **pz*$_4$lut** (pz* = 3,5-dimeththylpyrazolyl),

---

*To whom correspondence should be addressed. E-mail: james.gardinier@marquette.edu.

(1) Grohmann, A. *Adv. Inorg. Chem.* **2004**, *56*, 179.

(2) (a) Costas, M., Mehn, M. P., Jensen, M. P., Que, L., Jr. *Chem. Rev.* **2004**, *104*, 939 and references cited therein. (b) Kaizer, J.; Klinker, E. J.; Oh, N. Y.; Rohde, J.-U.; Song, W. J.; Stubna, A.; Kim, J.; Münck, E.; Nam, W.; Que, L., Jr. *J. Am. Chem. Soc.* **2004**, *126*, 472. (c) Jonas, R. T.; Stack, T. D. P. *J. Am. Chem. Soc.* **1997**, *119*, 8566. (d) Goldsmith, C. R.; Cole, A. P.; Stack, T. D. P. *J. Am. Chem. Soc.* **2005**, *127*, 9904.

(3) (a) Guerriero, P.; Vigato, P. A.; Fenton, D. E.; Hellier, P. C. *Acta Chem. Scand.* **1992**, *46*, 1025. (b) DeMott, J. C.; Basuli, F.; Kilgore, U. J.; Foxman, B. M.; Huffman, J. C.; Ozerov, O. V.; Mindiola, D. J. *Inorg. Chem.* **2007**, *46*, 6271.

(4) Huang, J.-S.; Xie, J.; Kui, S. C. F.; Fang, G.-S.; Zhu, N.; Che, C.-M. *Inorg. Chem.* **2008**, *47*, 5727.

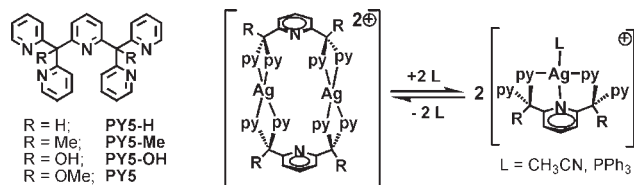(5) Morin, T. J.; Bennett, B.; Lindeman, S. V.; Gardinier, J. R. *Inorg. Chem.* **2008**, *47*, 7468.

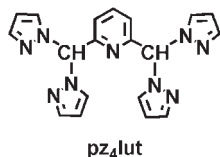**Figure 1. PY5-R** pentadentate ligand scaffolds and representative silver(I) complexes.

pz₄lut

Figure 2. pz₄lut pentadentate ligand.

and **pz^{DIP}₄lut** (pz^{DIP} = 3,5-diisopropylpyrazolyl), as well as the properties of their silver(I) complexes. Future reports will document the use of these ligands and their silver complexes in transition metal chemistry.

Experimental Section

General Considerations. The compound 2,6-pyridinedicarboxaldehyde was prepared according to the literature procedure.[6] While the preparation of **pz₄lut** has been described previously,[5] an improved preparation is described below along with additional characterization including the single-crystal X-ray structural determination. All other chemicals were commercially available and were used as received. Solvents were dried by conventional methods and distilled prior to use. The syntheses of the silver complexes were carried out under a nitrogen atmosphere using standard Schlenk techniques and in foil-covered apparatus to protect AgBF₄ or AgOTf from light. After complex formation, no special precautions to avoid light or air were taken.

Midwest MicroLab, LLC, Indianapolis, Indiana 45250, performed all elemental analyses. IR spectra were recorded for samples as KBr pellets in the 4000−500 cm^{-1} region on a Nicolet Magna-IR 560 spectrometer. ^{1}H and ^{13}C NMR spectra were recorded on a Varian 400 MHz spectrometer. Chemical shifts were referenced to solvent resonances at δ_H 7.26 and δ_C 77.23 for CDCl₃, δ_H 1.96 and δ_C 118.9 for CD₃CN. Details regarding diffusion NMR experiments are found in the Supporting Information. Absorption measurements were recorded on an Agilent 8453 spectrometer. Melting point determinations were made on samples contained in glass capillaries using an Electrothermal 9100 apparatus and are uncorrected. Mass spectrometric measurements recorded in ESI(+) mode were obtained on a Micromass Q-TOF spectrometer whereas those performed by using direct-probe analyses were made on a VG 70S instrument. For the ESI(+) experiments formic acid (approximately 0.1% v/v) was added to the mobile phase (CH₃CN). X-ray powder diffraction measurements were performed with a Rigaku MiniFlex II instrument using Cu Kα (1.54178 Å) radiation.

General Procedure for the Syntheses of pz^{R}₄lut Ligands. A solution of a given pyrazole, Hpz^R (6.1 equiv) in tetrahydrofuran (THF, ca. 0.3−0.7 M) was slowly added to a suspension of NaH (6 equiv) in THF at a rate to control hydrogen evolution. The resulting solution was stirred magnetically at room temperature for 30 min, then neat thionyl chloride (3 equiv) was slowly added by syringe (dropwise, to control the slightly

exothermic reaction) immediately causing the formation of copius colorless precipitate. After the mixture had been stirred at room temperature for 1 h, CoCl₂ (60 mol % of 2,6-pyridinedicarboxaldehyde) and 2,6-pyridinedicarboxaldehyde (1 equiv) were sequentially added as solids under a nitrogen blanket. The reaction flask was fitted with a condenser, and the mixture was heated at reflux 40 h under nitrogen. After cooling to room temperature, 50 mL of CH₂Cl₂ and 100 mL of 4 wt % NaHCO₃ and 1 wt % EDTA in water were added to the mixture. The layers were separated, and the aqueous phase was washed with three 50 mL portions of CH₂Cl₂. The combined organic layers were washed with two 100 mL portions of water, dried over MgSO₄, and filtered to give viscous pale orange or brown oils after removing solvent by rotary evaporation. The desired product was separated from the oily residue by column chromatography either on neutral alumina or on silica gel, as indicated below.

pz₄lut. The reaction between 3.00 g of (22.2 mmol) 2,6-pyridinedicarboxyaldehyde, 1.73 g of (13.3 mmol) CoCl₂, and 66.6 mmol O=S(pz)₂ in 400 mL of THF (formed in situ from 9.23 g of (135 mmol) pyrazole in 300 mL of THF, 3.20 g of (133 mmol) NaH in 100 mL of THF, and 4.84 mL of (7.92 g, 66.6 mmol) thionyl chloride) afforded 5.67 g of (69%) of **pz₄lut** as a colorless solid after aqueous workup and column chromatography of the oily product mixture on neutral alumina using Et₂O as the eluent and collecting the second band (R_f = 0.68 on a Al₂O₃ plate). Crystals suitable for X-ray diffraction were obtained by layering an acetone solution with hexanes and allowing solvents to diffuse 2 d. Both the powder and crystals had characterization data consistent with those previously reported.[5] Mp, 119−120 °C. ^{1}H NMR (CD₃CN, 293 K): δ 7.87 (t, J = 8 Hz, 1H, H₄-py), 7.83 (s, 2H, CH(pz)₂), 7.68 (d, J = 2 Hz, 4H, H₃-pz), 7.58 (d, J = 1 Hz, 4H, H₅-pz), 7.21 (d, J = 8 Hz, 2H, H$_{3,5}$-py), 6.35 (dd, J = 1; 2 Hz, 4H, H₄-pz). UV−vis (CH₃CN) λ$_{max}$, nm (ε, M^{-1}, cm^{-1}): 228 (33,000), 265 (8,500).

pz$^{4'}$₄lut. The crude product mixture obtained from a reaction between 0.459 g of (3.40 mmol) 2,6-pyridinedicarboxyaldehyde, 0.256 g of (2.04 mmol) CoCl₂, and 6.80 mmol O=S(pz$^{4'}$)₂ (formed in situ from 1.11 g of (13.5 mmol) 4-methylpyrazole in 50 mL of THF, 0.325 g of (13.5 mmol) NaH in 50 mL of THF, and 0.49 mL of (0.81 g, 6.8 mmol) thionyl chloride) was subject to column chromatography on neutral alumina. First, elution with Et₂O removed an unidentified impurity, then elution with ethyl acetate (R_f = 0.89, Al₂O₃ plate) afforded 1.05 g of (72%) of **pz$^{4'}$₄lut** as a colorless solid after removing solvent, triturating the oily fraction with Et₂O, and drying under vacuum. Mp, 145−148 °C. Anal. Calcd. (obsd.) for C₂₃H₂₅N₉: C, 64.62 (64.28); H, 5.89 (6.01); N, 29.49 (29.15). ^{1}H NMR (CDCl₃) δ_H 7.56 (t, J = 8 Hz, 1H, H₄-py), 7.36 (s, 2H, CH(pz$^{4'}$)₂), 7.21 (s, 4H, H₃-pz$^{4'}$), 7.11 (s, 4H, H₅-pz$^{4'}$), 6.95 (d, J = 8 Hz, 2H, H$_{3,5}$-py), 1.86 (s, 12H, CH₃). ^{1}H NMR (CD₃CN, 293 K) δ_H 7.82 (t, J = 8 Hz, 1H, H₄-py), 7.61 (s, 2H, CH(pz$^{4'}$)₂), 7.42 (s, 4H, H₃-pz$^{4'}$), 7.35 (s, 4H, H₅-pz$^{4'}$), 7.18 (d, J = 8 Hz, 2H, H$_{3,5}$-py), 2.03 (s, 12H, CH₃). ^{13}C NMR (CDCl₃) δ_C 154.8, 141.4, 138.6, 128.4, 122.8, 117.2, 78.1, 9.1. UV−vis (CH₃CN) λ$_{max}$, nm (ε, M^{-1}, cm^{-1}): 228 (33,000), 265 (8,500).

pz*₄lut. The crude product mixture obtained from a reaction between 3.40 g of (25.1 mmol) 2,6-pyridinedicarboxyaldehyde, 0.530 g of (4.10 mmol) CoCl₂ and 75.4 mmol O=S(pz*)₂ (formed in situ from 14.22 g of (147.9 mmol) 3,5-dimethylpyrazole in 200 mL of THF, 3.55 g of (147.9 mmol) NaH in 200 mL of THF, and 5.48 mL of (8.97 g, 75.4 mmol) thionyl chloride) was subject to column chromatography on neutral alumina. First, elution with Et₂O removed an unidentified impurity, then elution with ethyl acetate (R_f = 0.62, Al₂O₃ plate) afforded 5.44 g of (45%) of **pz*₄lut** as a colorless solid after removing solvent, triturating the oily fraction with Et₂O, and drying under vacuum. Mp, 156−157 °C. Anal. Calcd. (obsd.) for C₂₇H₃₃N₉: C, 67.06 (67.27); H, 6.88 (7.02); N, 26.07 (25.88). ^{1}H NMR

(6) (a) Luening, U.; Baumstark, R.; Peters, K.; Von Schnering, H. G. *Liebigs Ann. Chem.* **1990**, *2*, 129. (b) Steenland, M. W. A.; Lippens, W.; Herman, G. G.; Goeminne, A. M. *Bull. Soc. Chim. Belges* **1993**, *102*, 239.

(CDCl$_3$) δ_H 7.65 (t, J = 8 Hz, 1H, H$_4$-py), 7.41 (s, 2H, CH-(pz*)$_2$), 7.00 (d, J = 8 Hz, 2H, H$_{3,5}$-py), 5.78 (s, 4H, H$_4$-pz*), 2.15 (s, 12H, CH$_3$), 2.05 (s, 12H, CH$_3$). ^{1}H NMR (CD$_3$CN, 293 K) δ_H 7.75 (t, J = 8 Hz, 1H, H$_4$-py), 7.46 (s, 2H, CH(pz*)$_2$), 7.02 (d, J = 8 Hz, 2H, H$_{3,5}$-py), 5.87 (s, 4H, H$_4$-pz*), 2.10 (s, 12H, CH$_3$), 2.07 (s, 12H, CH$_3$). ^{13}C NMR (CDCl$_3$) δ_C 155.1, 148.3, 141.0, 137.7, 122.2, 106.7, 74.5, 13.8, 11.4. UV−vis (CH$_3$CN) λ_{max}, nm (ε, M^{-1} cm^{-1}): 228 (34,000), 267 (10,400).

pz$^{DIP}_4$lut. After aqueous workup of the reaction between 1.08 g of (25.1 mmol) 2,6-pyridinedicarboxaldehyde, 1.037 g of (7.99 mmol) CoCl$_2$ and O=S(pz^{DIP})$_2$ (formed in situ from 4.98 g of (32.7 mmol) 3,5-diisopropylpyrazole in 200 mL of THF, 0.790 g of (32.7 mmol) NaH in 200 mL of THF, and 1.13 mL of (1.90 g, 15.9 mmol) thionyl chloride), 5.79 g of brown oil was obtained. The ^{1}H NMR spectrum of the brown oil was consistent with a mixture of two main species, **pz$^{DIP}_2$lut** (90%) and 2-(pz$^{DIP}_2$CH)-6-[CH(O)]-C$_6$H$_3$N (10%). The composition of the mixture is determined using the relative integrations of resonances in the H$_4$-pz region of the spectrum at δ_H 5.86 (desired product) and δ_H 5.95 (monocarboxaldehyde). The comparable high solubilities of components prevented successful separation by column chromatography on either silica gel or alumina, therefore separation was achieved as follows: A 5.76 g (0.85 mmol) sample of the product mixture and 0.123 g of (0.85 mmol) 1,8-aminoquinoline in 15 mL of methanol was heated at reflux 1 h. This second product mixture was adsorbed onto a short pad of silica gel where elution with 4:1 hexanes/ethyl acetate (R_f = 0.64 SiO$_2$) gave 3.85 g (68% overall yield based on 2-pyridinedicarboxaldehyde) of **pz$^{DIP}_4$lut** as a tan solid after removing solvent, triturating with Et$_2$O, and drying under vacuum. Mp, 79−81 °C. Anal. Calcd. (obsd.) for C$_{43}$H$_{65}$N$_9$: C, 72.94 (72.86); H, 9.25 (9.11); N, 17.80 (17.89). ^{1}H NMR (CDCl$_3$) δ_H 7.66 (t, J = 8 Hz, 1H, H$_4$-py), 7.63 (s, 2H, CH(pz^{DIP})$_2$), 7.02 (d, J = 8 Hz, 2H, H$_{3,5}$-py), 5.86 (s, 4H, H$_4$- pz^{DIP}), 3.11 (sept, J = 7 Hz, 1H, ^{i}PrCH), 2.87 (sept, J = 7 Hz, 1H, ^{i}PrCH), 1.16 (d, J = 7 Hz, 24H, ^{i}PrCH$_3$), 0.91 (d, J = 7 Hz, 24 H, ^{i}PrCH$_3$). ^{1}H NMR (CD$_3$CN, 293 K) δ_H 7.76 (t, J = 8 Hz, 1H, H$_4$-py), 7.57 (s, 2H, CH(pz^{DIP})$_2$), 7.06 (d, J = 8 Hz, 2H, H$_{3,5}$-py), 6.02 (s, 4H, H$_4$- pz^{DIP}), 3.10 (sept, J = 7 Hz, 1H, ^{i}PrCH), 2.81 (sept, J = 7 Hz, 1H, ^{i}PrCH), 1.17 (d, J = 7 Hz, 24H, ^{i}PrCH$_3$), 1.03 (d, J = 7 Hz, 12 H, ^{i}PrCH$_3$), 0.97 (d, J = 7 Hz, 12 H, ^{i}PrCH$_3$). ^{13}C NMR (CDCl$_3$) δ_C 159.2, 156.5, 152.9, 138.6, 123.4, 100.8, 75.5, 30.8, 28.7, 26.3, 23.7 UV−vis (CH$_3$CN) λ_{max}, nm (ε, M^{-1} cm^{-1}), 205 (31,040), 221 (23,618sh), 265 (4941). Full details of the 2-(pz$^{DIP}_2$CH)-6-[CH(O)]-C$_6$H$_3$N derivative will be reported in more detail in elsewhere: ^{1}H NMR (CDCl$_3$) δ_H 9.96 (s, 1H, HC=O), 7.91 (ddd, J = 7.7, 1.2, 0.6 Hz, 1H, py), 7.85 (dd, J = 7.7, 1 Hz, 1H, py), 7.81 (s, 1H, CH(pz^{DIP})$_2$), 7.31 (ddd, J = 7.7, 1.2, 0.6 Hz, 1H, py), 5.95 (s, 2H, H$_4$- pz^{DIP}), 3.14 (sept, J = 7 Hz, 1H, ^{i}PrCH), 2.81 (sept, J = 7 Hz, 1H, ^{i}PrCH), 1.14 (d, J = 7 Hz, 3H, ^{i}PrCH$_3$), 1.12 (d, J = 7 Hz, 3H, ^{i}PrCH$_3$), 0.97 (d, J = 7 Hz, 3H, ^{i}PrCH$_3$), 0.95 (d, J = 7 Hz, 3 H, ^{i}PrCH$_3$).

[Ag(pz$_4$lut)](BF$_4$), 1. A solution of 0.500 g of (1.35 mmol) **pz$_4$lut** in 20 mL of THF was added to a solution of 0.262 g of (1.35 mmol) AgBF$_4$ in 15 mL of THF causing immediate precipitation. After the cloudy suspension had been stirred 4 h, the precipitate was isolated by cannula filtration, was washed with three successive 10 mL portions of Et$_2$O, and was dried under vacuum 12 h to give 0.663 g of (87%) **1** as a colorless powder. Mp, 210−214 °C (dec.) Anal. Calcd. (obsd.) for C$_{19}$H$_{17}$N$_9$AgBF$_4$: C, 40.31 (40.50); H, 3.03 (3.16); N, 22.27 (22.38). IR (KBr, cm^{-1}), ν(BF$_4^-$) regions: 1084, 1063, 775, 753. ^{1}H NMR (CD$_3$CN, 293 K) δ_H 7.94 (t, J = 8 Hz, 1H, H$_4$-py), 7.85 (s, 2H, CH(pz)$_2$), 7.84 (d, J = 2 Hz, 4H, H$_5$-pz), 7.61 (d, J = 1 Hz, 4 H, H$_3$-pz), 7.41 (d, J = 8 Hz, 2H, H$_{3,5}$-py), 6.36 (dd, J = 2, 1 Hz, 4H, H$_4$-pz), 2.16 (s, 26H, CH$_3$CN). ^{1}H NMR (CD$_3$CN, 233 K) δ_H 7.934 (t, J = 8 Hz, 1H, H$_4$-py), 7.927 (d, J = 2 Hz, 4H, H$_5$-pz), 7.85 (br s, 2H, CH(pz)$_2$), 7.57, (d, J = 1 Hz, 4H, H$_3$-pz), 7.29 (br s, 2H, H$_{3,5}$-py), 6.36 (dd, J = 2,1 Hz, 4H, H$_4$-pz), 2.39

(s, 26H, CH$_3$CN). UV−vis (CH$_3$CN) λ_{max}, nm (ε, M^{-1} cm^{-1}): 218 (35,500), 263 (7,200). HRMS [ESI(+), m/z] Calcd. (Obs) for C$_{38}$H$_{34}$N$_{18}$Ag$_2$BF$_4$, [Ag$_2$(pz$_4$lut = L)$_2$(BF$_4$)]$^+$, 1045.1351 (1045.1318). LRMS [ESI(+), m/z] (Int.) [assign.]: 1282 (0.1) [Ag$_3$L$_2$(BF$_4$)$_2$(CH$_3$CN)]$^+$, 1137 (1) [Ag$_3$L$_2$(Cl)$_2$]$^+$, 1045 (0.1) [Ag$_2$L$_2$(BF$_4$)]$^+$, 993 (3) [Ag$_2$L$_2$(Cl)]$^+$, 849 (17) [AgL$_2$]$^+$, 622 (24) [Ag$_2$L(Cl)]$^+$, 480 (100) [AgL]$^+$, 394 (31) [NaL]$^+$, 372 (35) [HL]$^+$, 304 (26) [L-Hpz]$^+$. Colorless crystals of unsolvated [Ag(**pz$_4$lut**)]-(BF$_4$) suitable for X-ray were grown by layering a methanol solution of AgBF$_4$ onto a CH$_2$Cl$_2$ solution of the ligand and allowing solvents to diffuse 3 d.

[Ag(pz$^{4'}_4$lut)](BF$_4$), 2. A solution of 0.531 g of (1.24 mmol) **pz$^{4'}_4$lut** in 10 mL of THF was added to a solution of 0.241 g of (1.24 mmol) AgBF$_4$ in 10 mL of THF causing immediate precipitation. After the mixture had been stirred 4 h, the precipitate was isolated by cannula filtration, was washed with three successive 10 mL portions of Et$_2$O, and was dried under vacuum 12 h to give 0.648 g of (84%) **2** as a colorless powder. Mp, 189−195 °C (dec to a black solid). Anal. Calcd. (obsd.) for C$_{23}$H$_{25}$-N$_9$AgBF$_4$: C, 44.40 (44.07); H, 4.05 (4.04); N, 20.26 (19.94). IR (KBr, cm^{-1}) ν(BF$_4^-$) regions: 1084, 778. ^{1}H NMR (CD$_3$CN, 293 K, see text) δ_H 7.94 (t, J = 8 Hz, 2H, H$_4$-py), 7.68 (br s, 12H, CH(pz$^{4'}$)$_2$ and H$_3$-pz$^{4'}$), 7.40 (d, J = 8 Hz, 4H, H$_{3,5}$-py), 7.39, (s, 8H, H$_5$-pz), 2.16 (s, 8H, CH$_3$CN), 2.04 (s, 24H, pzCH$_3$). ^{1}H NMR (CD$_3$CN, 233 K) δ_H 7.97 (t, J = 8 Hz, 2H, H$_4$-py), 7.75 (br s, 8H, H$_3$-pz$^{4'}$), 7.62(br s, 4H, CH(pz$^{4'}$)$_2$), 7.26, (s, 8H, H$_5$-pz), 7.09 (br s, 4H, H$_{3,5}$-py), 2.38 (s, 8H, CH$_3$CN), 2.03 (s, 24H, pzCH$_3$). UV−vis (CH$_3$CN) λ_{max}, nm (ε, M^{-1} cm^{-1}): 227 (36,300), 264 (9,300). HRMS [ESI(+), m/z] Calcd. (Obs) for C$_{46}$H$_{50}$N$_{18}$Ag$_2$BF$_4$, [Ag$_2$(pz$^{4'}$lut = L)$_2$(BF$_4$)]$^+$, 1155.2605 (1155.2616). LRMS [ESI(+), m/z] (Int.) [assign.]: 1390 (0.5) [Ag$_3$L$_2$(BF$_4$)$_2$(CH$_3$CN)]$^+$, 1245 (1) [Ag$_3$L$_2$(Cl)$_2$]$^+$, 1157 (6) [Ag$_2$L$_2$(BF$_4$)]$^+$, 1105 (4) [Ag$_2$L$_2$(Cl)]$^+$, 961 (33) [AgL$_2$]$^+$, 678 (22) [Ag$_2$L(Cl)]$^+$, 536 (100) [AgL]$^+$, 428 (22) [HL]$^+$, 346 (13) [L-Hpz$^{4'}$]$^+$. Colorless crystals were obtained by vapor diffusion of THF into a concentrated CH$_3$CN solution.

[Ag(pz*$_4$lut)](BF$_4$), 3. A solution of 0.506 g of (1.05 mmol) **pz*$_4$lut** in 10 mL of THF was added to a solution of 0.208 g of (1.07 mmol) AgBF$_4$ in 10 mL of THF causing immediate precipitation. After the mixture had been stirred 4 h, the precipitate was isolated by cannula filtration, was washed with three successive 10 mL portions of Et$_2$O, and was dried under vacuum 12 h to give 0.536 g of (85%) **3** as a colorless powder. Mp, 242−245 °C (decomp.). Anal. Calcd. (obsd.) for C$_{27}$H$_{33}$N$_9$-AgBF$_4$: C, 47.81 (47.66); H, 4.90 (4.81); N, 18.58 (18.53). IR (KBr, cm^{-1}) ν(BF$_4^-$) regions: 1084, 783. ^{1}H NMR (CD$_3$CN, 233 K, see text) δ_H 7.75 (t, J = 8 Hz, 2H, H$_4$-py), 7.27 (s, 4H, CH(pz*)$_2$), 6.79 (d, J = 8 Hz, 4H, H$_{3,5}$-py), 6.04 (s, 4H, H$_4$-pz*), 5.81 (s, 4H, H$_4$-pz*), 2.41 (s, 36H, CH$_3$CN), 2.37 (s, 12H, pz*CH$_3$), 2.30 (s, 12H, pz*CH$_3$), 1.81 (s, 12H, pz*CH$_3$), 1.62 (s, 12H, pz*CH$_3$). ^{1}H NMR (CD$_3$CN, 293 K) δ_H 7.77 (br t, J = 8 Hz, 2H, H$_4$-py), 7.28 (s, 4H, CH(pz*)$_2$), 6.82 (br s, 4H, H$_{3,5}$-py), 6.02 (br, 4H, H$_4$-pz*), 5.84 (br, 4H, H$_4$-pz*), 2.34 (br, 24H, pz*CH$_3$), 2.18 (s, 36H, CH$_3$CN), 1.84 (br, 24H, pz*CH$_3$) ^{1}H NMR (CD$_3$CN, 353 K) δ_H 7.83 (t, J = 8 Hz, H$_4$-py), 7.34 (s, 4H, CH(pz*)$_2$), 7.02 (d, J = 8 Hz, 4H, H$_{3,5}$-py), 5.97 (s, 8H, H$_4$-pz*), 2.34 (s, 24H, pz*CH$_3$), 1.97 (s, 36H, CH$_3$CN), 1.92 (s, 24H, pz*CH$_3$). UV−vis (CH$_3$CN) λ_{max}, nm (ε, M^{-1}, cm^{-1}): 216 (39,400), 266 (6,600). HRMS [ESI(+), m/z] Calcd. (Obs) for C$_{54}$H$_{66}$N$_{18}$Ag$_2$BF$_4$, [Ag$_2$(pz*$_4$lut = L)$_2$(BF$_4$)]$^+$, 1267.3859 (1267.3835). LRMS [ESI(+), m/z] (Int.) [assign.]: 1267 (0.1) [Ag$_2$L$_2$(BF$_4$)]$^+$, 1215 (0.4) [Ag$_2$L$_2$(Cl)]$^+$, 1076 (6) [AgL$_2$]$^+$, 734 (8) [Ag$_2$L(Cl)]$^+$, 592 (38) [AgL]$^+$, 546 (7) [Na(CH$_3$CN)L]$^+$, 506 (40) [NaL]$^+$, 484 (100) [HL]$^+$, 388 (7) [L-Hpz*]$^+$. Colorless crystals were obtained by vapor diffusion of THF into a concentrated CH$_3$CN solution.

[Ag(pz$^{DIP}_4$lut)](BF$_4$), 4. A solution of 0.518 g of (0.73 mmol) **pz$^{DIP}_4$lut** in 10 mL of THF was added to a solution of 0.142 g of (0.73 mmol) AgBF$_4$ in 10 mL of THF giving a cloudy solution.

The flask was covered in foil and allowed to stir overnight forming a small amount of precipitate. The solution was filtered and was concentrated to give an oily solid residue which was triturated with Et_2O and dried under vacuum to give 0.475 g (72%) of **4** as a colorless powder. Mp, 165−170 °C (decomp.). Anal. Calcd. (obsd.) for $C_{43}H_{65}N_9AgBF_4$: C, 57.21 (56.91); H, 7.25 (7.45); N, 13.96 (13.78). IR (KBr, cm^{-1}) $\nu(BF_4^-)$ regions: 1083, 708. ^{1}H NMR (CD$_3$CN, 233 K, see text) δ_H 7.76 (br s 2H, H$_4$-py), 7.59 (s, 8H, CH(pz^{DIP})$_2$), 6.99 (br s 4H, H$_{3,5}$-py), 6.17 (m, 8H), 2.99 (br d, 16H, ^{i}PrCH), 2.51 (t, J = 1 Hz, 48H, ipr), 0.68 (br m, 48H, ^{i}PrCH$_3$). ^{1}H NMR (CD$_3$CN, 293 K) δ_H 7.78 (br t, J = 8 Hz, 2H, H$_4$-py), 7.14 (s, 4H, CH(pz^{DIP})$_2$), 6.33 (br s, 4H, H$_{3,5}$-py), 6.11 (br s, 8H, H$_4$- pz^{DIP}), 2.98 (br s, 8H, ^{i}PrCH), 2.21 (s, 48H, ^{i}PrCH$_3$), 0.81 (br m, 48H, ^{i}PrCH$_3$). ^{1}H NMR (CD$_3$CN, 353 K) δ_H 7.83 (t, J = 8 Hz, 2H, H$_4$-py), 7.42 (s, 4H, CH-(pz^{DIP})$_2$), 6.91 (br s, 4H, H$_{3,5}$-py), 6.13 (s, 8H, H$_4$-pz), 3.08 (sept, J = 7 Hz, 8H ^{i}PrCH), 2.66 (br s, 8H, ^{i}PrCH), 2.00 (s, 24H, ^{i}PrCH$_3$), 1.18 (d, J = 7 Hz, 12H, ^{i}PrCH$_3$), 1.11 (d, J = 7 Hz, 12H, ^{i}PrCH$_3$). UV−vis (CH$_3$CN) λ_{max}, nm (ε, M^{-1}, cm^{-1}): 215 (25,700), 267 (5,000). LRMS [ESI(+), m/z] (Int.) [assign.]: 958 (0.7) [Ag$_2$L(Cl)]$^+$, 814 (21) [AgL]$^+$, 731 (10) [NaL]$^+$, 708 (100) [L]$^+$, 556 (10) [L-Hpz^{DIP}]$^+$, 355 (17) [H$_2$L]$^{2+}$, 279 (21) [H$_2$L-pz^{DIP}]$^{2+}$, 189 (0.4) [Ag(CH$_3$CN)$_2$]$^+$, 153 (7) [H$_2$pz^{DIP}]$^+$.

[Ag(pz$^{DIP}_4$lut)](SO$_3$CF$_3$), 5. A solution of 0.200 g of (0.28 mmol) pz$^{DIP}_4$lut in 10 mL of THF was added to a solution of 0.72 g of (0.28 mmol) AgSO$_3$CF$_3$ in 10 mL of THF giving a cloudy solution. The flask was covered in foil and allowed to stir overnight forming a large amount of white precipitate. The precipitate was collected by filtration, was washed with Et_2O (3 × 10 mL), and was dried under vacuum to give 0.195 g (72%) of **5** as a colorless powder. Mp, 204−208 °C (decomp.). Anal. Calcd. (obsd.) for $C_{44}H_{65}N_9AgF_3SO_3$: C, 53.75 (54.04); H, 6.82 (6.82); N, 13.12 (12.89). IR (KBr, cm^{-1}) $\nu(SO_3CF_3^-)$ regions: ν[SO$_3$(E)]: 1267 cm^{-1}; ν[SO$_3$(A$_1$)]: 1032 cm^{-1}; ν[CF$_3$(A$_1$)]: 1259 cm^{-1}; [CF$_3$(E)]: 1153 cm^{-1}. ^{1}H NMR (CD$_3$CN, 233 K, see text) δ_H 7.77 (br s, 2H), 6.99 (br s, 4H), 6.17 (br m, 10H), 2.94 (br d, 8H), 2.44 (s, 48H, ^{i}PrCH$_3$), 0.75 (br m, 48H, ^{i}PrCH$_3$). ^{1}H NMR (CD$_3$CN, 293 K) δ_H 7.80 (t, J = 7 Hz, 2H, H$_4$-py), 7.11 (s, 4H, CH(pz^{DIP})$_2$), 6.34 (br s, 4H, H$_{3,5}$-py), 6.13 (br, 8H, H$_4$-pz^{DIP}), 2.96 (br, 4H, H$_4$-pz^{DIP}), 2.20 (br, 24H, ^{i}PrCH$_3$), 0.80 (br m, 2H ^{i}PrCH$_3$). ^{1}H NMR (CD$_3$CN, 353 K) δ_H 7.83 (t, J = 8 Hz, 2H, H$_4$-py), 7.37 (s, 4H, CH(pz^{DIP})$_2$), 6.80 (t, J = 8 Hz, 4H, H$_{3,5}$-py), 6.13 (s, 8H, H$_4$- pz^{DIP}), 3.06 (sept, J = 7 Hz, 8H, ^{i}PrCH), 2.56 (br s, 8H), 2.12 (s, 48H, ^{i}PrCH$_3$), 1.19 (d, J = 7 Hz, 24H, ^{i}PrCH$_3$), 1.10 (d, J = 7 Hz, 24 H, ^{i}PrCH$_3$). UV−vis (CH$_3$CN) λ_{max}, nm (ε, M^{-1}, cm^{-1}), 214 (33,300), 268 (5,700). HRMS [ESI(+), m/z] Calcd. (Obs) for $C_{43}H_{65}N_9Ag$, [Ag(pz$^{DIP}_4$lut = L)]$^+$, 814.4414 (814.4430). LRMS [ESI(+), m/z] (Int.) [assign.]: 958 (0.4) [Ag$_2$L(Cl)]$^+$, 816 (0.8) [AgL]$^+$, 731 (0.3) [NaL]$^+$, 708 (100) [L]$^+$, 556 (0.8) [L-Hpz^{DIP}]$^+$, 355 (23) [H$_2$L]$^{2+}$, 279 (29) [H$_2$L-pz^{DIP}]$^{2+}$, 153 (0.9) [H$_2$pz^{DIP}]$^+$. Colorless crystals were obtained by vapor diffusion of THF into a concentrated CH$_3$CN solution.

Crystallography. X-ray intensity data from a colorless prism of pz$_4$lut, a colorless block of pz$^*_4$lut, a colorless prism of [Ag$_2$(μ-pz$_4$lut)$_2$](BF$_4$)$_2$ (**1**), a colorless block of [Ag$_2$(μ-pz$^{4'}_4$lut)$_2$]-(BF$_4$)$_2$·2CH$_3$CN (**2**·CH$_3$CN), a colorless block of [Ag$_2$-(μ-pz$^*_4$lut)$_2$](BF$_4$)$_2$·2CH$_3$CN (**3**·CH$_3$CN), and a colorless prism of [Ag(pz$^{DIP}_4$lut)](OTf)·CH$_3$CN·0.5Et$_2$O (**5**·CH$_3$CN·0.5Et$_2$O), were collected at 100(2) K with a Bruker AXS 3-circle diffractometer equipped with a SMART2[7] CCD detector (Cu Kα radiation, λ = 1.54178 Å). Raw data frame integration and Lp corrections were performed with SAINT+.[7] Final unit cell parameters were determined by least-squares refinement of 7898 reflections from the data set of pz$_4$lut, 4243 reflections from the

data set of pz$^*_4$lut, 7747 reflections from that of **1**, 9918 reflections from that of **2**·CH$_3$CN, 9857 reflections of **3**·CH$_3$CN, and 8431 reflections of **5**·CH$_3$CN·0.5Et$_2$O with I > $2\sigma(I)$ for each. Analysis of the data showed negligible crystal decay during collection in each case. Direct methods structure solutions, difference Fourier calculations and full-matrix least-squares refinements against F^2 were performed with SHELXTL.[8] Semiempirical absorption correction based on the multiple measurement of equivalent reflections was applied to the data of each pz$_4$lut and pz$^*_4$lut while numerical absorption corrections based on the real shapes of the crystals for **1**, **2**·CH$_3$CN, and **3**·CH$_3$CN were applied using SADABS.[9] The crystal of **5**·CH$_3$CN·0.5Et$_2$O represents a regular non-merohedral twin with two (almost) equal components related by a 180° rotation around x. An empirical absorption correction using TWINABS[9] was applied to the data of **5**·CH$_3$-CN·0.5Et$_2$O. All non-hydrogen atoms were refined with anisotropic displacement parameters. Hydrogen atoms were located and refined in the case of pz$^*_4$lut while in the remainder of cases were placed in geometrically idealized positions and included as riding atoms. The X-ray crystallographic parameters and further details of data collection and structure refinements are presented in Table 1.

Results

Syntheses. The pz$^R_4$lut ligands were prepared using a variation of the CoCl$_2$-catalyzed Peterson rearrangement reactions[10] between the appropriate di(pyrazolyl^R)sulfone and 2,6-pyridinedicarboxaldehyde as in Scheme 1A. We found that the use of an excess of di(pyrazolyl)sulfone (ca. 3:1 mol ratio versus the dialdehyde) leads to a dramatic improvement in the yield of pz$_4$lut (69%) compared to the previously reported stoichiometric (2:1) conditions (26%).[5] Three other new ligands pz$^{4'}_4$lut, pz$^*_4$lut, and pz$^{DIP}_4$lut were prepared in good yields by adopting a similar strategy. However, it is noted that the sterically demanding pz$^{DIP}_4$lut derivative required an additional step for purification, as the product is typically contaminated with variable amounts of 2-(pz$^{DIP}_2$CH)-6-[CH(O)]-C$_6$H$_3$N (monocarboxaldehyde) that cannot be separated by crystallization or chromatographic separation. Instead, the monocarboxaldehyde impurity is removed by condensation with 8-aminoquinoline to afford the much less soluble imine derivative which is then easily separated from the desired pz$^{DIP}_4$lut by column chromatography. The reaction between AgBF$_4$ and each of the pz$^R_4$lut ligands (Scheme 1B) in THF proceeds to give high yields of the complexes, [Ag(pz$^R_4$lut)](BF$_4$) (**1** for R = H; **2** for R = 4-Me, **3** for R = 3,5-Me$_2$), as hygroscopic solids indicated by elemental analyses. Once dried under vacuum, **1**−**3** are free of solvent and are insoluble in hydrocarbons, ethereal, and halogenated solvents. The unsolvated complexes, especially **1**, exhibit surprisingly low solubilities in polar solvents such as acetone, CH$_3$CN, and MeOH. For instance, their molar solubilities in acetonitrile increase in the order **1** (ca. 7 mM) < **3** (ca. 20 mM) < **2** (ca. 30 mM). The complexes are soluble in highly polar solvents such as

(7) *SMART APEX2 Version 2.1−4, SAINT+ Version 7.23a, and SA-DABS Version 2004/1*; Bruker Analytical Xray Systems, Inc.: Madison, WI, 2005.

(8) *TWINABS 2008/2*; Bruker Analytical Xray Systems, Inc.: Madison, WI, 2008.

(9) Sheldrick, G. M. *SHELXTL*, Version 6.12; Bruker Analytical X-ray Systems, Inc.: Madison WI, 2001.

(10) (a) The′, K. I.; Peterson, L. K. *Can. J. Chem.* **1973**, *51*, 422. (b) The′, K. I.; Peterson, L. K.; Kiehlman, E. *Can. J. Chem.* **1973**, *51*, 2448. (c) Peterson, L. K.; Kiehlman, E.; Sanger, A. R.; The′, K. I. *Can. J. Chem.* **1974**, *52*, 2367. (d) Reger, D. L.; Grattan, T. C.; Brown, K. J.; Little, C. A.; Lambda, J. J. S.; Rheingold, A. L.; Sommer, R. D. *J. Organomet. Chem.* **2000**, *607*, 120.

Table 1. Crystallographic Data Collection and Structure Refinement for **pz$_4$lut**, **pz*$_4$lut**, [Ag$_2$(μ-**pz$_4$lut**)$_2$](BF$_4$)$_2$ (**1**), [Ag$_2$(μ-**pz$^{4'}_4$lut**)$_2$](BF$_4$)$_2$·2CH$_3$CN (**2**·CH$_3$CN), and [Ag$_2$(μ-**pz*$_4$lut**)$_2$](BF$_4$)$_2$·2CH$_3$CN (**3**·CH$_3$CN) and [Ag(**pz$^{DIP}_4$lut**)](OTf)·CH$_3$CN·0.5Et$_2$O (**5**·CH$_3$CN·0.5Et$_2$O)

	pz$_4$lut	pz*$_4$lut	1	2·CH$_3$CN	3·CH$_3$CN	5·CH$_3$CN·0.5Et$_2$O
formula	C$_{19}$H$_{17}$N$_9$	C$_{27}$H$_{33}$N$_9$	C$_{38}$H$_{34}$Ag$_2$B$_2$F$_8$N$_{18}$	C$_{50}$H$_{56}$Ag$_2$B$_2$F$_8$N$_{20}$	C$_{58}$H$_{72}$Ag$_2$B$_2$F$_8$N$_{20}$	C$_{48}$H$_{68}$AgF$_3$N$_{10}$O$_{3.5}$S
formula weight	371.42	483.62	1132.19	1326.51	1438.72	1038.05
crystal system	orthorhombic	triclinic	monoclinic	monoclinic	triclinic	monoclinic
space group	$P2_12_12_1$	$P\bar{1}$	$P2_1/c$	$P2_1/n$	$P\bar{1}$	Cc
temp. [K]	100(2)	100(2)	100(2)	100(2)	100(2)	100(2)
a [Å]	7.30230(10)	9.5143(2)	10.17430(10)	10.6907(2)	11.0965(4)	16.1224(6)
b [Å]	16.4433(2)	9.6633(2)	13.7155(2)	20.7716(4)	12.8261(2)	29.4322(10)
c [Å]	45.2477(6)	14.0229(2)	15.9977(2)	13.5676(3)	13.1776(2)	23.6489(8)
α [deg]	90	88.9340(10)	90	90	118.0520(10)	90
β [deg]	90	83.6710(10)	102.5170(10)	103.5190(10)	103.8740(10)	108.111(2)
γ [deg]	90	89.6990(10)	90	90	92.6180(10)	90
V [Å^3]	5433.07(12)	1281.17(4)	2179.35(5)	2929.38(10)	1579.16(7)	10665.8(6)
Z	12	2	2	2	1	8
$D_{calcd.}$ [g cm^{-3}]	1.362	1.254	1.725	1.504	1.513	1.293
λ [Å] (Cu Kα)	1.54178	1.54178	1.54178	1.54178	1.54178	1.54178
μ.[mm^{-1}]	0.724	0.625	7.986	6.039	5.648	3.887
abs. correction	multiscan	multiscan	numerical	numerical	numerical	multiscan
$F(000)$	2328	516	1128	1344	736	4352
θ range [deg]	2.86 to 68.13	3.17 to 67.27	5.50 to 68.20	3.97 to 67.99	3.97 to 67.06	3.00 to 68.11
reflections collected	46051	10663	18195	24254	13173	53558
independent reflections	5569 (R_{int} 0.0260)	4227 (R_{int} 0.0230)	3877 (R_{int} 0.0117)	5164 (R_{int} 0.0122)	5190 (R_{int} 0.0181)	40241 (R_{int} 0.0546)
T_min/max	0.8808/0.9511	0.7410/0.9176	0.1203/0.3438	0.1962/0.2826	0.2734/0.5755	0.4864/0.7462
data/restraints/ parameters	5569/0/757	4227/0/471	3877/0/307	5164/0/472	5190/0/550	40241/21/1270
goodness-of-fit on F^2	1.022	1.045	1.041	0.999	1.025	1.032
$R1/wR2[I > 2\sigma(I)]^a$	0.0343/0.0809	0.0357/0.0867	0.0205/0.0520	0.0218/0.0598	0.0227/0.0577	0.0606/0.1545
$R1/wR2$ (all data)^a	0.0400/0.0833	0.0425/0.0902	0.0206/0.0521	0.0219/0.0599	0.0234/0.0581	0.0658/0.1596

$^a R1 = \sum||F_o| - |F_c||/\sum|F_o|, wR2 = [\sum w(|F_o| - |F_c|)^2/\Sigma w|F_o|^2]^{1/2}$.

Scheme 1. Preparation of pz$^R_4$lut Ligands and AgBF$_4$ Coordination Complexes
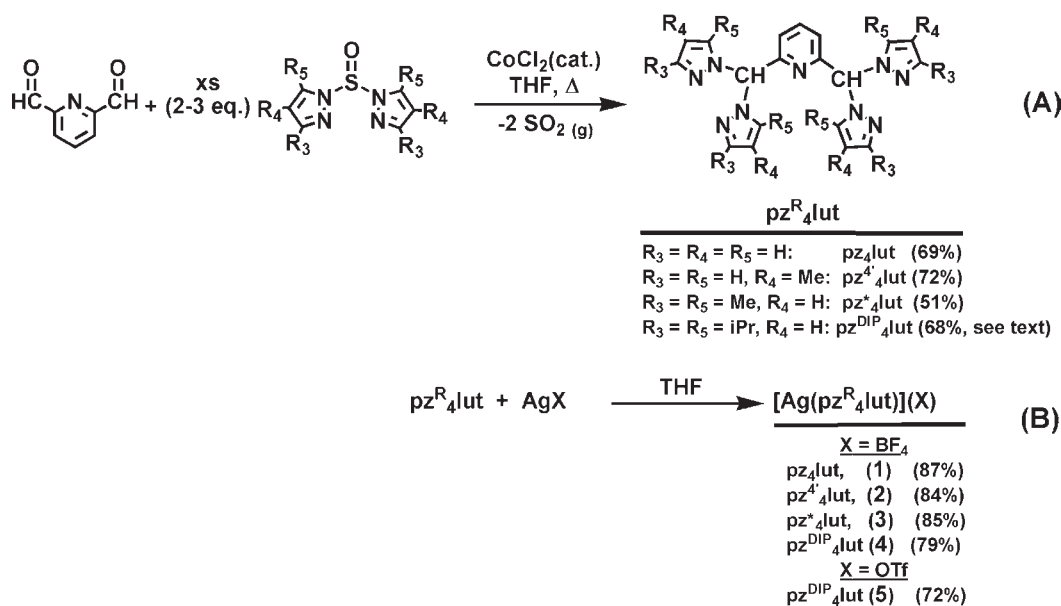
DMF or DMSO in which they are expected to be fully dissociated. In contrast to **1**−**3**, [Ag(**pz$^{DIP}_4$lut**)](X) (X = BF$_4$ (**4**), OTf (**5**)) are soluble in chlorinated solvents, acetone, CH$_3$CN, and MeOH. As with **1**−**3**, complexes **4** and **5** are insoluble in hydrocarbons and ethereal solvents.

Solid State Structures. Single crystals suitable for X-ray diffraction of the ligands **pz$_4$lut** and **pz*$_4$lut** were grown by layering acetone solutions with hexanes and allowing solvents to diffuse. The structural details (included here for completeness and for future reference) are provided in Table 1 and in the Supporting Information but will not be

further discussed. The silver complexes of the **pz$^{4'}_4$lut** and **pz*$_4$lut** ligands (**2**·CH$_3$CN and **3**·CH$_3$CN, respectively) were obtained by vapor diffusion of THF into dilute (ca. 10 mM) CH$_3$CN solutions. The silver complex of **pz$_4$lut** is too insoluble to afford X-ray quality crystals by this methodology as rapid precipitation affords only microcrystalline powder even from dilute solutions (vide infra). However, layering a methanol solution of AgBF$_4$ onto a CH$_2$Cl$_2$ solution of **pz$_4$lut** and allowing diffusion over 3 d was sufficient to obtain high quality crystals of unsolvated [Ag(**pz$_4$lut**)](BF$_4$) (**1**). Finally, we were not able to
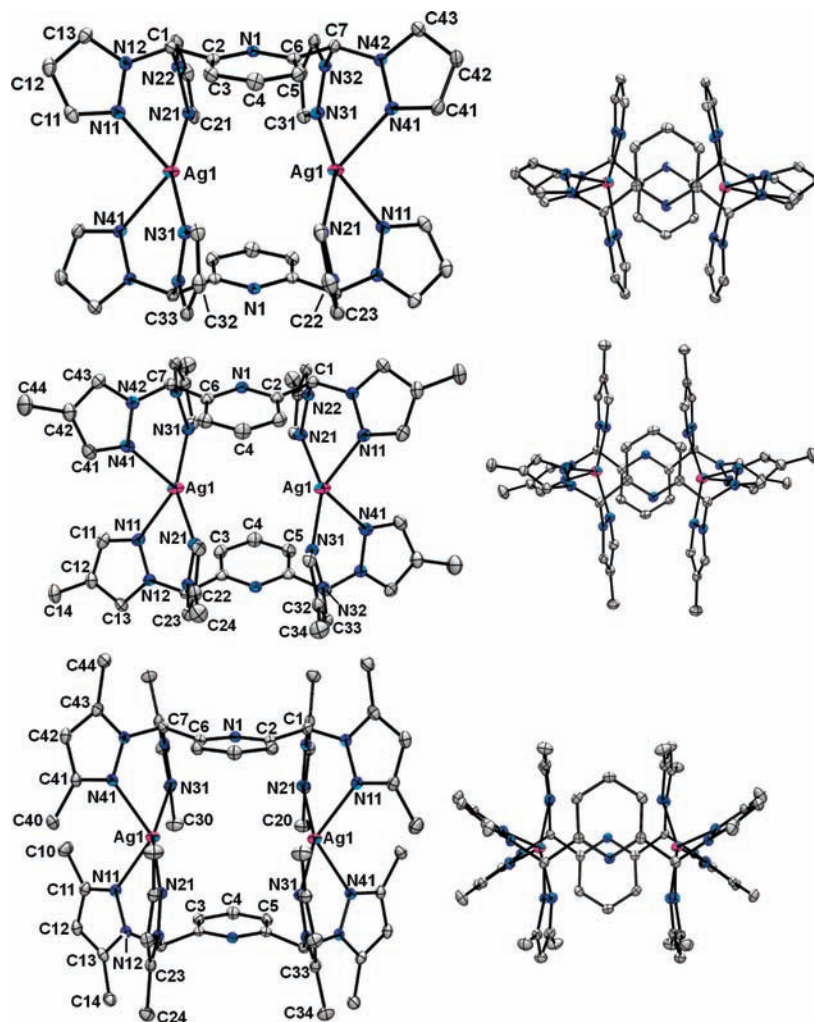
Figure 3. Views of the cyclic dications in [Ag(**pz₄lut**)](BF₄) (**1**), top; [Ag(**pz⁴'₄lut**)](BF₄)·CH₃CN, **2**·CH₃CN, middle; and [Ag(**pz*₄lut**)](BF₄)·CH₃CN, **3**·CH₃CN, bottom; Left, perspective view; Right, view normal to pyridyl plane. Each with thermal ellipsoids shown at 50% probability and with hydrogens removed for clarity.
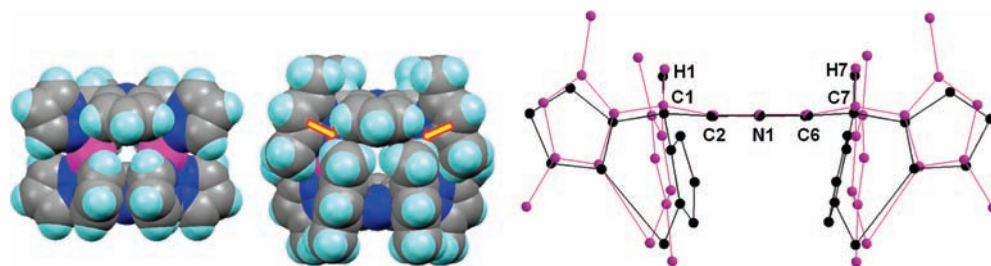

Figure 4. Space-filling representations of the crystal structures of cyclic dications of [Ag(**pz₄lut**)](BF₄), **1** (left), [Ag(**pz*₄lut**)](BF₄)·CH₃CN, **3**·CH₃CN (center), emphasizing the steric interactions involving the methyl and pyridyl groups of the latter. An overlay (right) shows greater bending of lutidine methines (C1 and C7) above the mean pyridyl plane containing N1 in **3** (pink) versus **1** (black).

obtain high quality crystals of [Ag(**pz^DIP₄lut**)](BF₄) (**4**) despite exhaustive attempts. Instead, either microcrystalline needles or, in one case with THF:CH₃CN, tiny blocks were obtained where all crystals exhibited bifringence under polarized light and did not hold their integrity when removed from solution. On the other hand, small twinned colorless prisms of [Ag(**pz^DIP₄lut**)](OTf)·CH₃CN·0.5Et₂O (**5**·CH₃CN·0.5Et₂O) were obtained by vapor diffusion of Et₂O into a CH₃CN solution. The small, twinned nature of the crystals and the disorder of solvents and anions contribute to the rather low quality of

the structure, but the results are sufficient to establish the connectivity. The structures of the cations in **1**, **2**·CH₃-CN, and **3**·CH₃CN are provided in Figures 3 and 4 while that of **5**·CH₃CN·0.5Et₂O is found in Figure 5. Selected intra-cation bond distances and angles are collected in Table 2.

As can be seen in Figure 3, complexes **1**−**3** each contain a cyclic bimetallic dication (of nearly ideal C_{2h} symmetry) that is located on an inversion center. In each dication, the two silver centers are well-separated (4.77−5.39 Å) by the bridging, chelating ligand. Each silver center possesses a
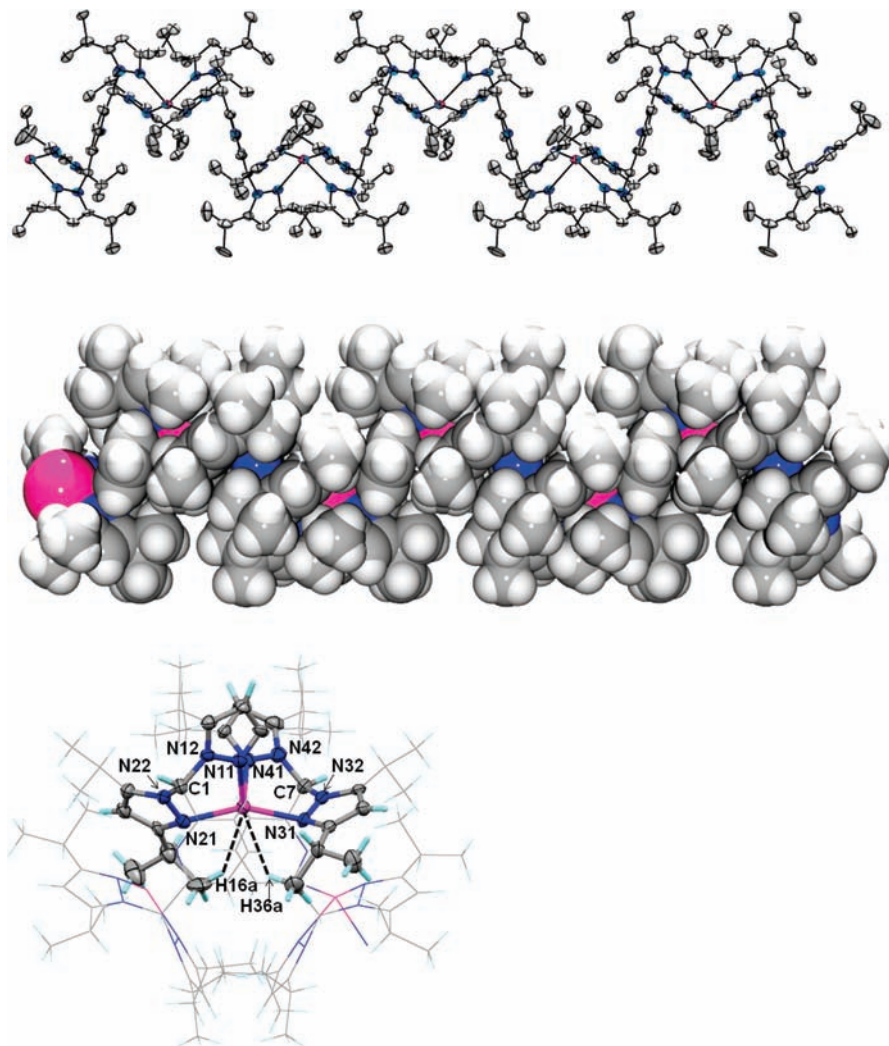
Figure 5. Views of the cation in [Ag(**pz$^{DIP}_4$lut**)](OTf)·CH$_3$CN·0.5Et$_2$O (**5**·CH$_3$CN·0.5Et$_2$O). Top: ORTEP drawing (thermal ellipsoids shown at 50% probability and with hydrogens removed for clarity) of a fragment of one polymeric chain that propagates along *a*-axis. Middle: Space-filling representation of same fragment. Bottom: A view approximately down the *a*-axis emphasizing the coordination environment about silver.

slightly distorted seesaw geometry imposed by disparate bonding to pyrazolyl nitrogens that occupy either pseudo-axial or pseudo-equatorial positions about the metal (the central pyridyl remains unbound). Thus, there are two shorter, nearly collinear pseudo-axial Ag−N bonds, Ag1−N21 and Ag1−N31, that average 2.215 Å for **1**, 2.244 Å for **2**·CH$_3$CN, and 2.256 Å for **3**·CH$_3$CN with N21−Ag1−N31 of 156° for **1**, 152° for **2**·CH$_3$CN, and 158° for **3**·CH$_3$CN. The other two pseudo-equatorial Ag−N bonds, Ag−N11 and Ag1−N41, are longer (averaging 2.412 Å for **1**, 2.374 Å for **2**·CH$_3$CN, and 2.431 Å for **3**·CH$_3$CN) than the pseudo-axial bonds. The corresponding N11−Ag−N41 bond angles are more acute (103° for **1**, 106° for **2**·CH$_3$CN, and 114° for **3**·CH$_3$CN) than the pseudo-axial N21−Ag1−N31 angle. The average of the four Ag−N distances (2.334 Å for **1**, 2.309 Å for **2**·CH$_3$CN, and 2.323 Å for **3**·CH$_3$CN) and ligand bite angles (corresponding to N11−Ag1−N21 and N31−Ag1−N41 which are 84° for **1**, 85° for **2**·CH$_3$CN, and 80° for **3**·CH$_3$CN) are all in line with those found in

the closely related dications of [Ag$_2$(μ-*m*-[CH(pz)$_2$]$_2$-C$_6$H$_4$)$_2$](X)$_2$ (X = BF$_4$, PF$_6$)[11] or [Ag$_2$(μ-[CH(pz)$_2$]$_2$-(CH$_2$)$_n$)$_2$]$^{2+}$ (*n* = 1−3)[12] and indicate that the influence of anions, central linker, or, surprisingly, even the addition of methyl groups at the 3- and 5- positions of the pyrazolyls have little influence on the metal's primary coordination geometry. On the other hand, the added steric bulk of 3-methyl groups in **3**·CH$_3$CN relative to **1** causes van der Waals contacts with the central pyridyl rings (Figure 4) that distort the cyclic dication by bending the lutidyl methines C1 and C7 in **3**·CH$_3$CN on average 0.25 Å above the mean plane of the pyridyl rings (Figure 4, right). For comparison, the C1 and C7 atoms of **1** reside, on average, only 0.07 Å above the mean plane of the pyridyl. Similarly, the corresponding methine atoms in [Ag$_2$(μ-*m*-[CH(pz)$_2$]$_2$C$_6$H$_4$)$_2$]]$^{2+}$ are also only displaced by 0.07 Å.[11]

In light of the steric interactions in **3**, it was anticipated that bulkier groups on the pyrazolyls would break the cyclic motif. Indeed, in complex **5** the cation is no longer

(11) Reger, D. L.; Watson, R. P.; Smith M. D. *Inorg. Chem.* **2006**, *45*, 10077 and references.

(12) Reger, D. L.; Watson, R. P.; Gardinier, J. R.; Smith, M. D. *Inorg. Chem.* **2004**, *43*, 6609.

Table 2. Selected Interatomic Bond Distances (Å), Bond Angles (deg), and Bond Torsion Angles (deg) for [Ag(**pz₄lut**)](BF₄) (**1**), [Ag(**pz⁴′₄lut**)](BF₄)·CH₃CN, **2**·CH₃CN, [Ag(**pz*₄lut**)](BF₄)·CH₃CN, **3**·CH₃CN, and [Ag(**pz^DIP₄lut**)](OTf)·CH₃CN·0.5Et₂O (**5**·CH₃CN·0.5Et₂O)

	1	**2**·CH₃CN	**3**·CH₃CN	**5**·CH₃CN· 0.5Et₂O
Distances (Å)				
Ag1−N11	2.4284(15)	2.4121(15)	2.3855(17)	2.373
Ag1−N21	2.2154(15)	2.2617(14)	2.3030(16)	2.238
Ag1−N31	2.2139(16)	2.2485(15)	2.3002(16)	2.249
Ag1−N41	2.4329(16)	2.4106(16)	2.3894(16)	2.356
Ag···Ag	4.767(2)	4.956(2)	5.391(2)	8.628, 8.610
Bond Angles (deg)				
N11−Ag1−N21	85.76(5)	84.91(5)	79.92(6)	86.98
N31−Ag1−N41	83.10(5)	85.09(5)	81.09(6)	86.14
N11−Ag1−N41	103.32(5)	106.23(5)	114.27(5)	91.93
N21−Ag1−N31	155.99(6)	151.77(5)	157.89(6)	155.23
N11−Ag1−N31	107.45(5)	116.07(5)	113.39(6)	110.49
N21−Ag1−N41	113.94(5)	107.98(5)	110.38(6)	111.49
Torsion Angles (deg)				
Ag1N11−N12C1	18.3(2)	9.8(2)	0.2(2)	21.77
Ag1N21−N22C1	−23.8(2)	−28.8(2)	−15.8(2)	−49.83
Ag1N31−N32C7	−16.6(2)	−24.9 (2)	−28.6(2)	−44.39
Ag1N41−N42C7	9.3(2)	12.2(2)	0.8(2)	20.99
H1C1−C2N1	71.9(2)	−64.8	−75.6(2)	67.95
H7C7−C6N1	−70.8(2)	71.5	72.3	70.37

cyclic but is organized into polymeric chains that propagate along the crystallographic *a*- axis (Figure 5). The complex contains an unbound pyridyl as in **1**−**3** but, in contrast to the three latter complexes, the silver-bound dipyrazolylmethane units are located on opposite sides of the central pyridyl ring; the H1C1−C2N1 and H7C7−C6N1 torsion angles (Table 2) have the same sign in **5** but have opposite signs in **1**−**3**. On first inspection, the distorted seesaw coordination environment about silver in **5** appears similar to those in **1**−**3** in that the shorter pseudo-axial Ag−N bonds (avg. 2.244 Å), longer pseudo-equatorial Ag−N bonds (avg. 2.365 Å), and average Ag−N bond length of 2.304 Å (indicative of tetra-coordinate silver[13]) are all similar to those distances found in **1**−**3**. However, while the pseudo-axial N21−Ag−N31 angle of 155° is in line with those in **1**−**3**, the pseudo-equatorial N11a−Ag-N41 angle of 92° is more acute than those in **1**−**3**. Closer inspection of the silver coordination sphere shows that opposite to the N11a−Ag-N41 fragment, there are two rather short Ag···H contacts Ag···H26dC26 (2.603 Å, 139°) and Ag···H36aC36 (2.788 Å, 134°) that arise from methyls of the 3-isopropylpyrazolyl groups. An additional consequence of the moderate steric profiles of the isopropyl-pyrazolyl substituents is that there is substantial twisting of pyrazolyl rings defined by the absolute value of the AgN-NC_methine torsion angle (Table 5). Pyrazolyl ring twisting is a common distortion in metal poly(pyrazolyl)methane complexes[14] and provides one measure of the 'fit' of these ligands to the metal (and vice versa); ideally this value should be zero. For **5**, the average pyrazolyl ring twist of 34° is much greater than 17°, 19°, and 11° found in **1**−**3**,

respectively, where it is noted that in all cases the pseudo-axial rings are more twisted than the pseudo-equatorial rings. The greater pyrazolyl ring twisting in **5** likely arises from the several intrachain van der Waals contacts involving the isopropyl substituents and neighboring pyridyl and pyrazolyl rings.

As detailed in the Supporting Information, the highly organized supramolecular structures of **1**−**3** likely contribute to the low solubilities of the compounds. That is the crystal packing of **1**−**3** is dominated by numerous noncovalent interactions including CH···F weak hydrogen bonding involving the tetrafluoroborate and acidic hydrogens of pyridyl and pyrazolyl rings as well as various CH-π and π−π stacking interactions involving heterocyclic aromatic groups. In **5**, the isopropyl substituents protect aromatic groups from entering into extensive 'intermolecular' noncovalent interactions (being limited only to CH···O weak hydrogen bonding). The relative number of noncovalent interactions identified in each crystal parallels the observed trend in solubility (**1** < **3** < **2** ≪ **5**). It is important to note, however, that aside from **1**, the structures obtained from single crystal X-ray structural determination may not be representative of the bulk crystalline solid. For illustration, the X-ray powder diffraction patterns obtained from various samples of **1** and **3** are given in Figure 6. The structure of **1** obtained by single crystal diffraction did not contain any solvent in the lattice. Accordingly, both the powder initially isolated from the reaction mixture (Figure 6, top left) in THF and the samples of ground vacuum-dried crystals grown by layering MeOH and CH₂Cl₂ solutions (Figure 6, middle left) showed identical diffraction patterns that were consistent with the calculated pattern obtained from the single crystal structure determination. On the other hand, the structure of **3** from single crystal X-ray diffraction showed it to be a CH₃CN solvate, but elemental analysis of vacuum-dried samples indicated that solvent is absent. The diffraction patterns for as-isolated (dried and ground) powder from the preparative reaction and that of a bulk sample after recrystallization (after vacuum-drying and grinding) were identical. Fittingly, neither pattern was consistent with that calculated for **3**·CH₃CN from the single crystal X-ray diffraction experiment. Single crystals become opaque and fracture upon drying. Thus, it would seem desolvation significantly alters the structure. As detailed in the Supporting Information, similar observations hold for **2** and **5**, but desolvation causes loss of crystallinity in the latter case.

Solution Properties. For complexes **1**−**5**, the combined data from electrospray ionization mass spectrometric (ESI-MS) as well as variable temperature and diffusion ¹H NMR spectroscopic measurements suggest that the solid state structures are not maintained in CH₃CN solution. Instead, monometallic cations are most likely the predominant species in the liquid temperature range of CH₃CN. ESI-MS data are thought to accurately reflect the solution structures of coordination complexes and coordination polymers of inert metals.[15] For labile silver(I)

(13) Liddle, B. J.; Hall, D.; Lindeman, S. V.; Smith, M. D.; Gardinier, J. R. *Inorg. Chem.* **2009**, *48*, 8404.

(14) Reger, D. L.; Gardinier, J. R.; Elgin, J. D.; Smith, M. D.; Hautot, D.; Long, G. L.; Grandjean, F. *Inorg. Chem.* **2006**, *45*, 8862.

(15) (a) Miras, H. N.; Wilson, E. F.; Cronin, L. *Chem. Commun.* **2009**, 1297. (b) Baytekin, B.; Baytekin, H. T.; Schalley, C. A. *Org. Biomol. Chem.* **2006**, *4*, 2825.
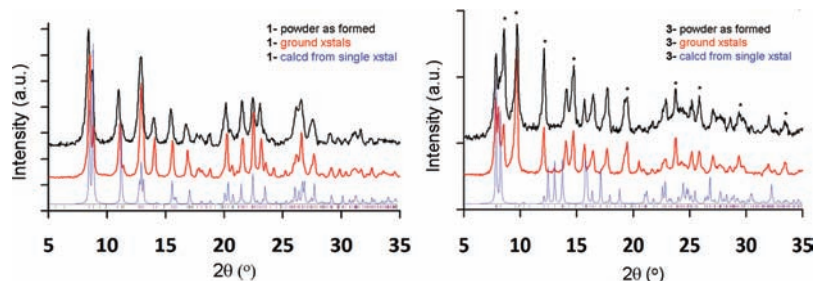
Figure 6. X-ray powder diffraction patterns of **1** (left) and **3** (right) obtained for initially obtained precipitate of preparative reactions in THF (top, black) and for bulk crystalline samples (middle, red) after drying and grinding. The calculated diffraction patterns based on single crystal diffraction experiments are also given (bottom, blue). For **3**, reflections demarcated with asterices (*) are not found in the calculated pattern of the solvate **3·CH₃CN**.
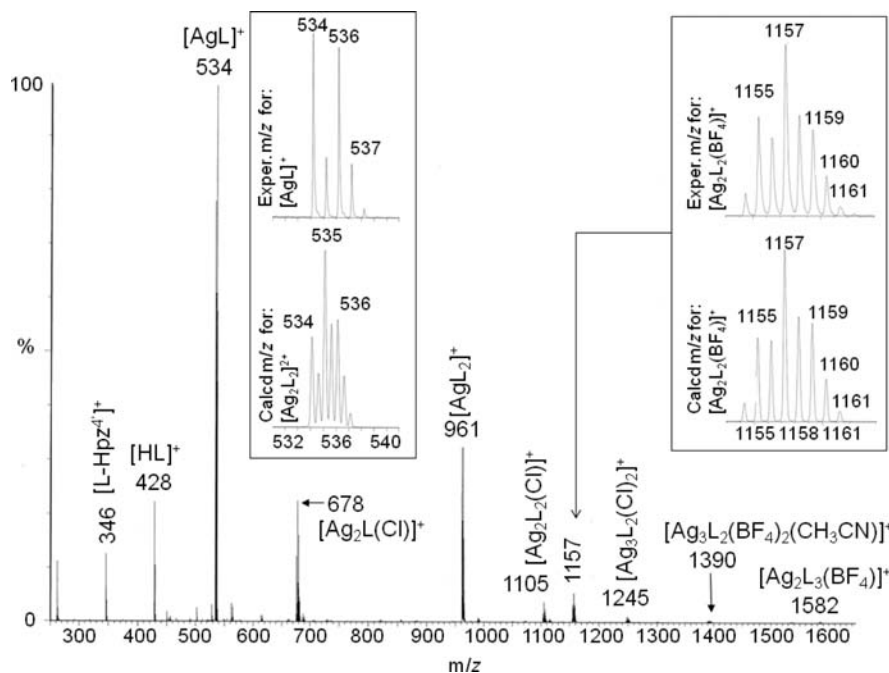

Figure 7. ESI(+)- mass spectrum of [Ag($pz^{4'}_4lut$)](BF₄), **2** in CH₃CN.

complexes such as with polytopic di(pyrazolyl)methane ligands linked via various organic spacers and of related ligands,[11−13,16,17] ESI-MS data appear to provide reliable measure for distinguishing which complexes will form metallacycles versus coordination polymers in the solid state. For instance, it has been reported that those complexes that give cyclic dications in the solid state such as either $[Ag_2(\mu\text{-}m\text{-}[CH(pz)_2]_2C_6H_4)_2](X)_2$ (X = BF₄, PF₆)[11] or $[Ag_2(\mu\text{-}[CH(pz)_2]_2(CH_2)_n)_2]^{2+}$ ($n = 1-3$)[12] give a weak peak in their ESI(+) mass spectrum with m/z corresponding to $[Ag_2L_2(X)]^+$ (X = anion) whereas such a peak is absent in cases where the solid state structure is of a coordination polymer. In the latter cases, very weak intensity peaks for higher order species such as $[Ag_3L_2\text{-}(X)_2]^+$ are sometimes observed. In all previously reported cases, the ESI(+) spectrum contains peaks for $[AgL_2]+$ and $[AgL]^+$ (the base peak is never for $[Ag_2L_2]^{2+}$ from the easily distinguishable isotope patterns, middle of Figure 7). In many cases, peaks for $[HL]^+$, $[HL\text{-}pz]^+$,

$[AgL(CH_3CN)]^+$, and $[Ag(CH_3CN)_n]^+$ ($n = 1-4$) are observed. All of the above observations demonstrate that ambiguity still exists concerning whether the ESI-MS data of silver(I) complexes accurately reflects their solution structures, and the current study serves to further probe this issue. The ESI(+)-MS data for **1−5** are in general agreement with findings for the related aryl- or alkylidene linked di(pyrazolyl)methane ligands but some important differences are also observed. First, as in the above-mentioned related cases, weak intensity peaks for $[Ag_2L_2(X)]^+$ (X = BF₄⁻, and Cl⁻ from the spectrometer) were observed for **1** and **2** (for example, m/z = 1105 and 1157 in Figure 7) which showed cyclic dications in the solid state, but such peaks were absent in the spectrum of **4** or **5**. Interestingly, the $[Ag_2L_2(X)]^+$ peak in the spectrum **3** was only observed at relatively high concentration even though the solid state structure was also of a cyclic dication. Second, very weak intensity peaks for higher-order $[Ag_2L_3(X)]^+$ and $[Ag_2L_2(X)_2]^+$ ions were observed for **1** and **2** but not for **3−5** which would seem to indicate that **1** and **2** form coordination polymers to some small extent either in solution or during the desolvation phase of the mass spectrometry experiment. The lack of higher order peaks for **5** (and **4**) is rather surprising given the

(16) Reger, D. L.; Gardinier, J. R.; Grattan, T. C.; Smith, M. R.; Smith, M. D. *New J. Chem.* **2003**, *27*, 1670.
(17) (a) Gwengo, C.; Silva, R. M.; Smith, M. D.; Lindeman, S. V.; Gardinier, J. R. *Polyhedron* **2009**, *362*, 4127. (b) Silva, R. M.; Smith, M. D.; Gardinier, J. R. *Inorg. Chem.* **2006**, *45*, 2132.

Table 3. Summary of Results from PFGSE ^{1}H NMR Experiments

compound	D ($\times 10^{-11}$ m^2/s)	r_H (Å, PFGSE)	X-ray radius^a (Å)	modeled radius^b (Å, HF 3-21G or PM3)
Ga(acac)$_3$	10.6	4.84	4.84[20]	
pz$_4$lut	9.18	5.57	6.20	5.34
pz$^{4'}_4$lut	8.86	5.77		6.10
pz*$_4$lut	8.05	6.35	6.73	6.24
pz$^{DIP}_4$lut	6.23	8.21		7.30
[Ru(bpy)$_2$(CH$_3$CN)$_2$]$^{2+}$	8.94	5.72	5.72[21]	5.95
1	8.88	5.76	7.46	6.10 monomer max., 7.40 dimer
2	8.64	5.92	7.77	7.50 monomer max., 8.60 dimer
3	8.13	6.29	7.89	7.32 monomer max., 7.94 dimer
4	6.33	8.08		8.90 ML, 9.2 ML$_2$
5	5.76	8.88	7.61, 9.70, 10.14 AgL, AgL$_2$, Ag$_2$L$_3$	8.90 ML, 9.2 ML$_2$

^{a} From largest measured hydrogen−hydrogen distance, see text. ^{b} Largest measured hydrogen−hydrogen distance was used. Also, because parameters for silver are not available for PM3 in SPARTAN08,[22] monomeric silver complexes were modeled by adding K$^+$ near, but not bound, to ligand and minimizing energy

solid state coordination polymer structure. It is also of interest that higher-order ions were not reported for the related [Ag$_2$(μ-m-[CH(pz)]$_2$C$_6$H$_4$)$_2$](X)$_2$ (X = BF$_4$, PF$_6$).[11] The spectrum for each **1−5** contains peaks for [AgL$_2$]$^+$, [Ag$_2$L(Cl)]+, [AgL]$^+$, [HL]$^+$, and [L-Hpz]$^+$ where [AgL]$^+$ is the base peak for **1** and **2** while [HL]$^+$ is the base peak for **3−5**. The spectrum for each **1−3** contains a peak for [AgL$_2$]$^+$, a species absent in the spectrum of either **4** or **5**. It is noteworthy that a peak corresponding to [AgL-(CH$_3$CN)]$^+$ is absent in the spectra of **1−5**. Such a species was conjectured to exist for **PY5-R** derivatives in solution, but a peak was also absent in the reported mass spectral data.[4] Regardless, the presence of peaks for multiple silver ions with different numbers of **pz$^R_4$lut** ligands in the corresponding spectrum of each **1−5** would seem to indicate significant dissociation occurs in solution, a conjecture that is supported by NMR spectral data.

The NMR spectral data from a variety of different experiments including variable temperature ^{1}H and pulsed field-gradient spin−echo[18] (PFGSE) NMR studies of each **1−5** indicate that these complexes are monomeric in CD$_3$CN solution. The resonances for the metal-bound ligands in **1−5** are distinct from the respective "free" ligand resonances both by their downfield chemical shifts and by their temperature dependence. The appearance of the ^{1}H NMR spectrum of each **1−5** in CD$_3$CN under various conditions is itself suggestive of monomeric [AgL]$^+$ ions in solution. If the solid state structures of **1−3** and **5** were retained in solution (and if **1−3** had ideal C_{2h} symmetry), two sets of resonances for symmetrically distinct (pseudo-axial and pseudo-equatorial) pyrazolyl group hydrogens would be expected, but only one set is observed for each complex **1−5** at about ambient temperature or above. For "intact" cyclic dications of **1−3**, a minimum of two Ag−N(pz) bonds would need to be broken concomitant with multiple C−C and C−N bond rotations for pseudo-axial and pseudo-equatorial pyrazolyl groups to give exchange-averaged signals; a highly improbable scenario relative to the dynamic processes available to monomeric cations. The variable temperature NMR studies of each **1−5** over the liquid range of CD$_3$CN, fully detailed in the Supporting Information, indeed showed quite low activation

barriers toward pyrazolyl exchange of about 10 kcal/mol for complexes **1−2** and of about 14 kcal/mol for complexes **3−5**. These low activation barriers are reminiscent of restricted C−C or C−N bond rotations in molecular multipropellors and aromatic propellenes [tri(aryl)methanes or poly(pyrazolyl)arenes][19] and lend further support for the monomeric nature of the complexes at room temperature and above. Finally, the PFGSE NMR experiment permits the indirect evaluation of molecular size by monitoring changes in signal intensity incurred through varying axial field gradients.[18] Smaller species diffuse more readily and cause greater signal loss on increasing field gradient than larger species. The slopes of plots of signal intensity versus gradient field strength gives diffusion coefficients which, after application of the Stokes−Einstein relation, afford hydrodynamic radii. The typical uncertainty in the PFGSE experiments is such that for ideal, non-interacting reference compounds, the hydrodynamic radii are typically within 10−15% of those radii found from X-ray diffraction studies. A summary of results of PFGSE NMR experiments of room temperature CD$_3$CN solutions of ligands with Ga(acac)$_3$ added as an internal reference and of individual silver complexes, **1−5**, each with [Ru(bpy)$_2$-(CH$_3$CN)$_2$](BF$_4$)$_2$ added as an internal reference are found in Table 3, Figure 8 and in the Supporting Information. The viability of this method was first demonstrated using the ligands described here, where the hydrodynamic radii were found to be slightly smaller but comparable to the crystallographic radii or to those radii obtained from energy-minimized structure calculations (HF 3-21G). For complexes **1−3**, the hydrodynamic radii more closely match calculated values for monomeric cations estimated from semiempirical (PM3) geometry optimizations than those values for dimeric dications obtained from either single-crystal X-ray diffraction

(18) (a) Valentini, M.; Pregosin, P. S.; Rüegger, H. *Organometallics* **2000**, *19*, 2551. (b) Stilbs, P. *Prog. NMR Spectrosc.* **1987**, *19*, 1.
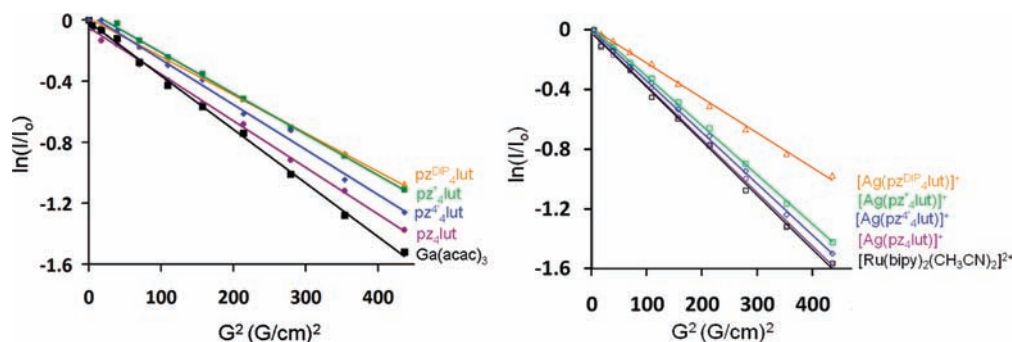
(19) Molecular multipropellers: (a) Mislow, K. *Acc. Chem. Res.* **1976**, *9*, 26–33. (b) Sedó, J.; Ventosa, N.; Molins, M. A.; Pons, M.; Rovira, C.; Veciana, J. *J. Org. Chem.* **2001**, *66*, 1579–1589. (c) Vicente, J.; Chicote, M.-T.; Lagunas, M.-C.; Jones, P. G.; Ahrens, B. *Inorg. Chem.* **1997**, *36*, 4938–4944. (d) For leading references, of aromatic propellenes, see: Foces-Foces, C.; Llamas-Saiz, A.; Fernández-Castaño, C.; Claramunt, R. M.; Escolástico, C.; Lavandera, J. L.; Santa María, M. D.; Jimeno, M. L.; Elguero, J. *J. Chem. Soc., Perkin Trans. 2* **1997**, 2173.

(20) Dymock, K.; Palenik, G. J. *Acta Crystallogr., Sect. B* **1974**, *30*, 1364.

(21) Heeg, M. J.; Kroener, R.; Deutsch, E. *Acta Crystallogr., Sect. C* **1985**, *41*, 684.

(22) *SPARTAN'08*; Wavefunction, Inc.: Irvine, CA

Figure 8. Results from PFGSE ^{1}H NMR experiments.

experiments or molecular modeling calculations. Similarly, the hydrodynamic radii for **4** and **5** are consistent with monomeric $[AgL]^+$ species rather than with radii for $[AgL_2]^+$, dimers such as $[Ag_2L_2]^{2+}$ or even higher-order oligomers such as $[Ag_2L_3]^{2+}$ or $[Ag_3L_4]^{3+}$ (values that can be extracted from the crystal structure of polymeric **5** or from molecular modeling).

Summary and Conclusions

A series of ligands based on the tetra(pyrazolyl)lutidine scaffold with alkyl-groups of differing steric profiles decorating the pyrazolyl units have been prepared. The silver(I) complexes of these ligands have also been prepared where it was noted that the surprisingly poor solubility of the complexes even in polar aprotic organic solvents such as CH_3CN can be improved with increasing alkyl substitution because of two main factors: (*i*) alkyl groups reduce the number of noncovalent interactions between ions and (*ii*) in the case of *iso*-propyl groups, there is a drastic change in solid state structure when compared to the other complexes. The *iso*-propyl substituents enforce a polymeric chain structure owing to steric interactions between the alkyls and the central pyridyl ring (in addition to protecting the cation scaffold from extensive noncovalent interactions). With less bulky or with no alkyl groups on the pyrazolyl rings, cyclic bimetallic dicationic motifs replete with extensive noncovalent interactions are found. It was demonstrated by X-ray powder diffraction that the silver(I) complex of **pz$_4$lut** formed directly

from the preparative reaction is structurally identical to the bulk sample after recrystallization and to that used for the single crystal diffraction experiment. In the other cases, the bulk powder formed directly from the preparative reactions and the vacuum-dried bulk recrystallized sample are structurally equivalent but are different from the observed crystal structure, likely because of differences in solvation. Despite the differences in solid state structures, the cumulative solution NMR and ESI(+) mass spectral data of each silver(I) complex indicate that they are monomeric once dissolved in acetonitrile and undergo dynamic intra- and intercationic exchange processes. Unfortunately, the labile nature of the exchange processes renders the solution structures ambiguous (which would remain true even if the solid state structures of monomeric species were known). Nonetheless, despite the rather low solubility of the silver-(I) complexes, their facile ligand exchange has been helpful for further developing the transition metal coordination chemistry of these ligands, results to be reported imminently.